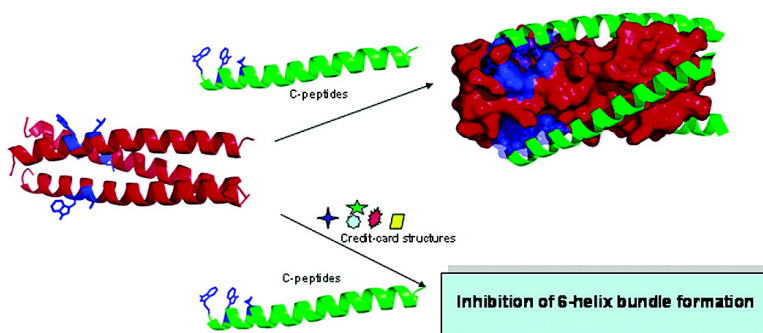


Evaluation of “Credit Card” Libraries for Inhibition of HIV-1 gp41 Fusogenic Core Formation

Yang Xu, Hong Lu, Jack P. Kennedy, Xuxia Yan, Laura A. McAllister, Noboru Yamamoto, Jason A. Moss, Grant E. Boldt, Shibo Jiang, and Kim D. Janda

J. Comb. Chem., **2006**, 8 (4), 531-539 • DOI: 10.1021/cc0600167 • Publication Date (Web): 22 April 2006

Downloaded from <http://pubs.acs.org> on March 22, 2009



More About This Article

Additional resources and features associated with this article are available within the HTML version:

- Supporting Information
- Links to the 1 articles that cite this article, as of the time of this article download
- Access to high resolution figures
- Links to articles and content related to this article
- Copyright permission to reproduce figures and/or text from this article

[View the Full Text HTML](#)



ACS Publications
 High quality. High impact.

Evaluation of “Credit Card” Libraries for Inhibition of HIV-1 gp41 Fusogenic Core Formation

Yang Xu,[†] Hong Lu,[‡] Jack P. Kennedy,[†] Xuxia Yan,[‡] Laura A. McAllister,[†]
Noboru Yamamoto,[†] Jason A. Moss,^{†,§} Grant E. Boldt,[†] Shibo Jiang,[‡] and
Kim D. Janda^{*,†}

Department of Chemistry and Immunology and The Skaggs Institute for Chemical Biology and Worm Institute for Research and Medicine (WIRM), The Scripps Research Institute, 10550 North Torrey Pines Road, La Jolla, California 92037, and Laboratory of Viral Immunology, the Lindsey F. Kimball Research Institute, The New York Blood Center, 310 East 67th Street, New York, New York 10021

Received February 10, 2006

Protein–protein interactions are of critical importance in biological systems, and small molecule modulators of such protein recognition and intervention processes are of particular interest. To investigate this area of research, we have synthesized small-molecule libraries that can disrupt a number of biologically relevant protein–protein interactions. These library members are designed upon planar motif, appended with a variety of chemical functions, which we have termed “credit-card” structures. From two of our “credit-card” libraries, a series of molecules were uncovered which act as inhibitors against the HIV-1 gp41 fusogenic 6-helix bundle core formation, viral antigen p24 formation, and cell–cell fusion at low micromolar concentrations. From the high-throughput screening assays we utilized, a selective index (SI) value of 4.2 was uncovered for compound **2261**, which bodes well for future structure activity investigations and the design of more potent gp41 inhibitors.

Introduction

The necessity for therapeutically viable small-molecule inhibitors of HIV-1 infection remains as pressing as ever. In the past decade, increased knowledge of viral entry mechanisms has opened the door to the discovery of clinically useful HIV-1 entry inhibitors.^{1–5} Such molecules can intercept the virus before it invades the cell, unlike most drugs currently in use, which act only after infection occurs.^{6,7} HIV-1 entry inhibitors could also be used as prophylactic agents to assemble a barrier against the initial infection. There are a number of protein molecules involved in the viral entry process, on both the host cell and on the virus, providing multiple protein targets for intervention. The viral transmembrane glycoprotein gp41 is of particular interest due to its critical role in viral fusion.^{8–10}

The HIV-1 virus enters a target cell by fusion of the viral envelope and the cell membrane, followed by release of viral genetic material into the cell. This process is mediated by viral envelope (Env) glycoproteins gp120 and gp41, both derived from precursor protein gp160.¹¹ The glycoproteins gp120 and gp41 associate noncovalently to form a quaternary trimeric structure in the viral prefusogenic form, whereas fusion of the virion with the target cell is triggered by gp120 binding to the CD4 cell surface protein¹² and then to one of a group of chemokine co-receptors on CD4+ target cells,

such as CXCR4 or CCR5.¹³ This ligand–receptor binding induces a conformational change in gp120, which thereby converts gp41 to its fusogenic form.⁸ This cascade of conformational changes positions the gp41 fusion peptide in close proximity to the target cell membrane, leading to viral entry. The gp41 subunit of the HIV-1 Env glycoprotein therefore plays a critical role in mediating viral entry and presents a promising target for the development of viral fusion inhibitors.

The gp41 protein subunit consists of 345 amino acid residues with a molecular weight of 41 kDa, whereas SIV gp41 has a MW of 44 kDa (Scheme 1a). The ectodomain of gp41 contains a fusion peptide region marked by both hydrophobic and glycine-rich regions, as well as heptad repeats. These heptads are located adjacent to the N- and C-terminal portions and are designated NHR and CHR, respectively. In the native (i.e., nonfusogenic) state, the fusion peptide is buried in the gp120/gp41 quaternary complex. Upon gp120 binding to CD4 and a co-receptor, the conformational change in gp41 orients the fusion peptide toward the host cell membrane via a “spring-loaded” mechanism similar to the low pH-induced influenza hemagglutinin HA₂-mediated membrane fusion process.⁸ The fusion peptide region is followed by the NHR and CHR terminal regions, which consist of hydrophobic residues predicted to form α -helical coiled coils. These regions likely mediate the oligomerization and conformational change of gp41 into its fusogenic state. The NHR region is located adjacent to the fusion peptide, whereas the CHR region precedes this transmembrane segment.

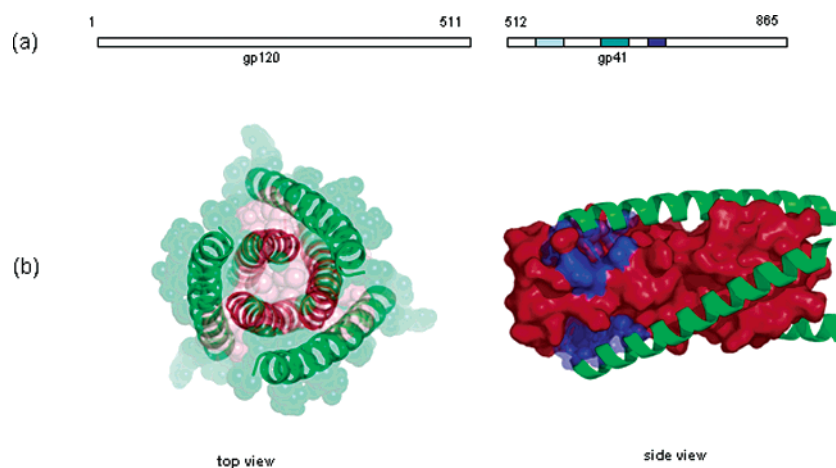
* To whom correspondence should be addressed. kjanda@scripps.edu.

[†] The Scripps Research Institute.

[‡] New York Blood Center.

[§] Present address: C S Bio Co., 20 Kelly Court, Menlo Park, CA 94025.

Scheme 1



(a) Primary structure of gp120 and gp41; (b) X-ray crystallography structure of fusogenic gp41². Pink color highlights the N-terminal trimeric structure; green color highlights C-terminus; blue color highlights the prominent binding pocket for small-molecule fusion inhibitors.

Protein dissection studies, as well as X-ray crystallography, have revealed that the NHR and CHR regions of gp41 co-associate to form a helical trimer of antiparallel dimers in the fusion-active gp41 core domain.^{2,14,15} The inner coiled-coil trimer is formed by the leucine zipperlike heptad repeat sequence, whereas the outer trimer of C-helices packs in an antiparallel fashion into the grooves on the surface of the inner trimer (Scheme 1B). The C-helix interacts with the N-helix through hydrophobic amino acid residues located in the grooves of the N-helix trimer; these amino acid residues are highly conserved in most HIV-1 viral strains. Molecules that impede the formation of the six-helix bundle could terminate this fusogenic transformation and thereby preclude viral fusion. This hypothesis has been supported by findings that externally added N- and C-terminal peptide fragments of gp41 can inhibit the fusion of HIV-1 or HIV-1-infected cells to uninfected cells.^{16–18} A gp41 C-terminal peptide, DP178, also known as Enfuvirtide and Fuzeon, is currently in clinical use for treating HIV-1 infection.¹⁹ In a recent study, Bianchi et al. have demonstrated that a covalently stabilized HIV gp41 N-terminal peptide trimer, (CCIZN17)₃, is the most potent fusion inhibitor known to date (IC₅₀ = 40–380 pM).²⁰ While the search for peptide-based fusion inhibitors has been successful, the identification of small molecule HIV viral fusion inhibitors remains elusive. However, this difficulty notwithstanding, the search for small-molecule inhibitors is of enormous importance given that small-molecule therapeutics almost invariably exhibit improved pharmacokinetic profiles, oral bioavailability, and vastly simpler synthesis scale-up on the manufacturing scale relative to synthetic peptide-based therapeutics.^{9, 10}

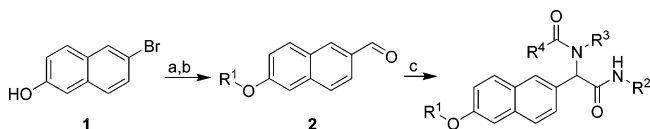
In an effort to discover small-molecule inhibitors targeting gp41 fusogenic activation, Ferrer et al. have generated a biased combinatorial chemical library of nonnatural binding elements aimed at disruption of the gp41 core association.²¹ From this library, small molecules were identified that, when covalently attached to a peptide from the gp41 N-terminal peptide, inhibit gp41-mediated cell fusion. Along a similar vein, Jiang et al. recently identified a series of small molecules that block the gp41 fusogenic core formation and inhibit HIV fusion.²² Using molecular docking techniques,

Jiang et al. screened a database of 20 000 organic molecules and found 16 compounds that present a good fit into the hydrophobic cavity within the gp41 core, as well as maximum possible interactions within the target binding site. Following further examination, two of these compounds, ADS-J1 and ADS-J2, displayed inhibitory activity at micromolar concentrations against the formation of the gp41 core structure and on HIV-1 infectivity.¹⁰ A notable corroboration of the therapeutic viability of small-molecule fusion inhibitors is a recent study from the same group, which revealed that the flavin derivatives in black tea and catechin derivatives in green tea inhibit HIV-1 entry also by targeting gp41.²³

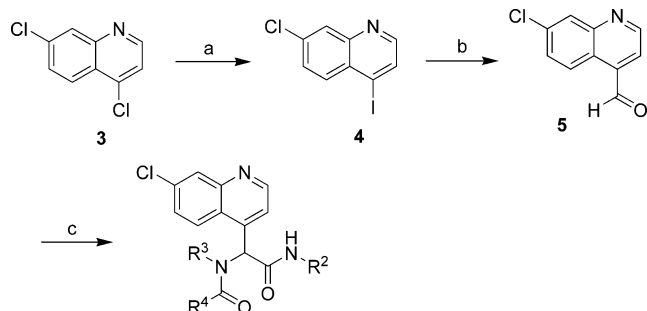
We have recently begun exploring the ability of what we have termed “credit card” libraries to disrupt protein–protein interactions of biological relevance.^{24,25} The chemical structures of these libraries are grounded upon flat, rigid scaffolds, adorned with functionalities that span a wide range of size, polarity, aromaticity, and hydrogen-bonding capability. The rationale for the design of the library scaffold is based on the concept of the “hot spot”—a region in protein–protein interfaces that are rich in aromatic residues and contribute to the stability of the overall quaternary structure.^{26,27} It is our hypothesis that interactions at a hot spot can be disrupted with planar, aromatic compounds that compete for binding and, therefore, may efficiently disrupt the assembly. Applying this logic, we have demonstrated that credit card libraries possess members that disrupt c-Myc–Max interactions, a dimerization event that is responsible for tumorigenesis in many types of human cancers.²⁴ Furthermore, with the aid of computational refinement, molecules from this same library have been uncovered as inhibitors against acetylcholinesterase-induced β -amyloid aggregation.²⁵ Herein, we report the identification of compounds from two credit card libraries that inhibit the HIV-1 gp41 fusogenic core formation and HIV-1 replication.

Results

Synthesis of Chemical Libraries. The credit card libraries were centered upon scaffolds displaying planar, aromatic core structures, such as naphthalene and quinoline. The Ugi four-component condensation (4CC) reaction was utilized to

Scheme 2. Synthesis of “Credit Card” Library I Based on a Naphthalene Scaffold^a

^a Reagents: (a) ^tBuLi (2 equiv), THF, -78 °C, then DMF; (b) R¹Br, K₂CO₃, DMF, 60 °C; (c) R²NC, R³NH₂, R⁴CO₂H, MeOH/CHCl₃, reflux.

Scheme 3. Synthesis of “Credit Card” Library II Based on a Quinoline Scaffold^a

^a Reagents: (a) TMSI, NaI, Propionitrile, 90 °C; (b) ^tBuLi (2 equiv), THF, -78 °C, then DMF; (c) R²NC, R³NH₂, R⁴CO₂H, MeOH/CHCl₃, reflux.

introduce functional diversity to the general α -acylamino amide core, whereas a wide range of structural elements were introduced through variation of size, polarity, aromaticity, and hydrogen-bonding capability.

In total, each compound in the naphthalene-based library was synthesized in either two or three steps (Scheme 2). Thus, lithiation of 6-bromo-2-naphthol **1**, followed by quenching with DMF, afforded the general building block 6-hydroxy-2-naphthaldehyde, which was then treated with a variety of alkyl halides to yield the corresponding phenolic ethers **2**. To diversify this scaffold, a mixture of compound **2**, isocyanides (R²NC), amines (R³NH₂), and carboxylic acids (R⁴CO₂H) were reacted in a parallel fashion to assemble the final α -acylamino amide structure by the Ugi 4CC reaction.^{28,29} Overall, 285 individual molecules were prepared in modest to high yields (30–90%) and excellent purity (>95%) after chromatographic purification. We also note that each compound was prepared in racemic form for the purpose of screening studies.

To further evaluate the planar region of the “credit card” library molecular scaffold, a quinoline heterocycle, Scheme 3, was also utilized as the aldehyde constituent in the Ugi 4CC. Thus, for credit-card library II, 4,7-dichloroquinoline **3** was treated with iodotrimethylsilane to obtain the chemo-selective iodination product **4**. After a selective iodo lithiation and treatment with DMF, the aldehyde **5** was isolated in good yield posed for the Ugi 4CC reaction. For the synthesis of library II, **5** was subjected to the Ugi 4CC reaction with a range of isocyanides, amines, and carboxylic acids to grant our second library. A total of 118 molecules were prepared as racemates, and individually purified at high purities (>95%).

Library Selection for the Inhibition of Fusogenic gp41 Core Formation and HIV-1-Mediated Syncytium Formation. Both libraries were screened for gp41 fusogenic core formation inhibition activity using a highly sensitive assay,

the sandwich enzyme-linked immunosorbent assay (ELISA), in which the six-helix bundle (6-HB) formed by N36 and C34 was captured by rabbit polyclonal antibodies and detected by a mouse mAb, termed NC-1, which specifically recognizes the discontinuous epitopes on this quaternary complex. The sandwich ELISA was first established by Jiang et al. to specifically identify small molecule HIV-1 inhibitors that target gp41.³⁰ The advantage of this assay is its promiscuous detection of all “hits” that block six-helix bundle formation, irrespective of inhibitor binding site(s). After screening both libraries at 10 μ M per member, we identified 10 compounds with $\geq 50\%$ inhibition, including **2293**, **1032**, **299**, **2300**, **1046**, **2278**, **2249**, **2261**, **1004**, and **2D6**. Interestingly, **2D6** from library II was found to be the Passerini adduct and not the expected Ugi 4CC product. The Passerini reaction is a three-component condensation reaction between a carboxylic acid, a carbonyl compound and an isocyanide.^{31,32} Passerini adducts, α -hydroxy carboxamides, are often observed as byproducts in Ugi 4CC reactions because they share three common reaction components. The Passerini product **2D6** formation in our study can be attributed to the postulation that the *tert*-butylamine component is too bulky to form the Schiff base with the aldehyde **5** efficiently in the early stage of the condensation reaction, a key step for Ugi 4CC reaction, but not for Passerini 3CC reaction; therefore, Passerini 3CC adduct, **2D6**, was produced as the main product for this particular reaction. Excitingly, inhibition was still observed in the six-helix bundle assay using **2D6**. This further suggests the planar core does, indeed, play a major role for the inhibition of protein–protein interactions.

Concurrently, libraries I and II were screened for inhibition of HIV-1-mediated syncytium formation, which is complementary in allowing the detection of HIV-1 induced cell–cell fusion. In this process, one HIV-1 infected cell fuses with multiple uninfected cells to form a syncytium, which is defined as a cell having more than four nuclei and balloon. Strikingly, all the active compounds (*vide supra*) except **2249** inhibited syncytium formation at 10 μ M. From this initial screen, nine molecules emerged from library I and a single molecule was identified from library II; these structures are shown in Figure 1.

The Inhibitory Activity of the Preselected Compounds as Judged by gp41 Six-Helix Bundle Formation, HIV-1-Mediated Cell–Cell Fusion and HIV-1 Replication. The 10 preselected compounds were further examined for their inhibitory activity on the gp41 six-helix bundle formation, HIV-1-mediated cell–cell fusion, and HIV-1 replication using enzyme immunoassay (EIA), dye transfer, and p24 assays, respectively. In the EIA assay, N36 peptide was first preincubated with a selected compound at graduated concentrations, followed by addition of biotinylated C34 peptide.^{4,33} The mixture was then added to a 96-well polystyrene plate precoated with the mAb NC-1. After incubation, SA-HRP and TMB were added sequentially. Absorbance at 450 nm was measured as described (*vide infra*) and used to calculate the concentration for 50% inhibition (IC₅₀) of six-helix bundle formation. The dye transfer assay is the most rapid screening method for assessing HIV-1-mediated cell–cell fusion, usually requiring only a few hours.³⁴ In this assay,

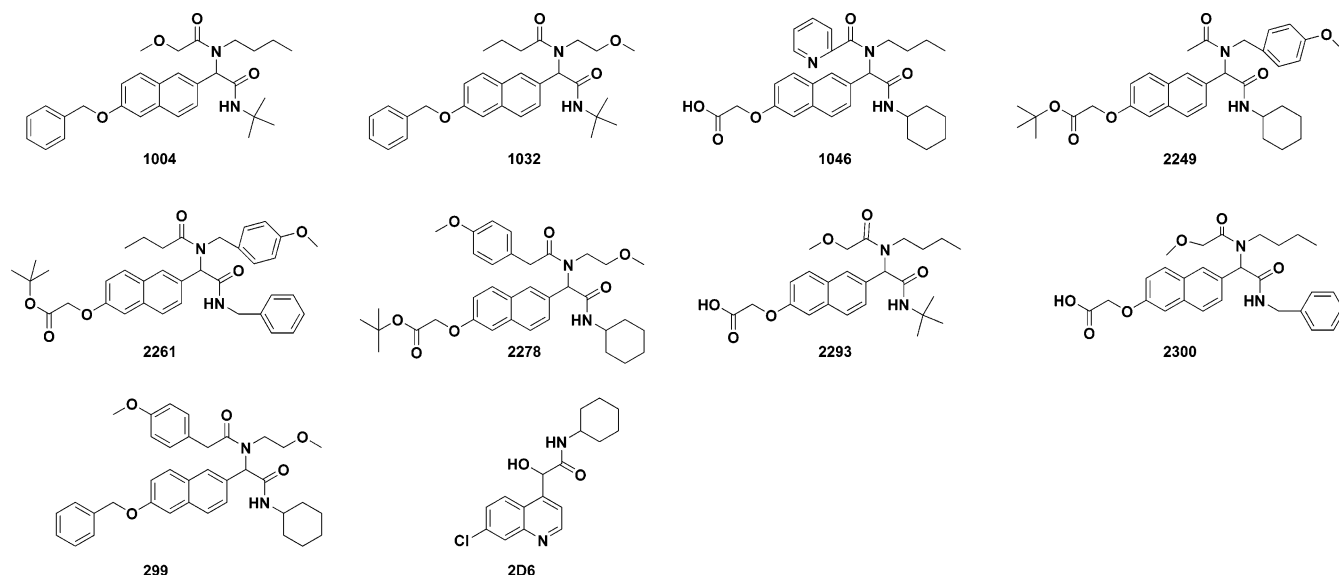


Figure 1. Compounds preselected from the sandwich ELISA and sycytium formation assays.

Table 1. Inhibitory Activities of the Preselected Compounds on HIV-1-Mediated Cell–Cell Fusion and HIV-1 Replication

compd	MW	IC ₅₀ ^a for inhibition of 6-HB formation (μM)	IC ₅₀ for inhibition of cell–cell fusion (μM)	IC ₅₀ for inhibition of p24 production (μM)	CC ₅₀ ^b (μM)	SI ^c
2293	458.55	23.42 ± 0.71 ^d	— ^e	—	>80	NA
1032	490.63	25.73 ± 0.04	—	18.5 ± 2.5	48.0 ± 0.5	2.6
299	594.74	35.19 ± 2.29	—	—	>80	NA
2300	492.56	42.13 ± 4.18	—	—	>80	NA
1046	517.62	33.20 ± 5.60	—	—	>80	NA
2278	618.76	29.93 ± 14.94	—	44.5 ± 7.4	45.4 ± 6.7	1.0
2249	574.71	36.59 ± 2.67	—	19.4 ± 4.9	43.6 ± 1.6	2.3
2261	610.74	38.26 ± 2.19	—	11.3 ± 2.5	47.5 ± 1.0	4.2
1004	490.63	42.32 ± 6.99	40.5 ± 1.2	16.8 ± 3.1	40.5 ± 0.9	2.4
2D6	318.80	47.34 ± 2.72	15.3 ± 1.2	—	35.4 ± 1.6	NA

^a IC₅₀: 50% inhibitory concentration. ^b CC₅₀: 50% cytotoxic concentration. ^c Selectivity index (SI) = CC₅₀/IC₅₀ for inhibiting p24 production. ^d Mean ± SD. ^e “—” indicates <50% inhibition or no detectable inhibitory activity at 80 μM due to cytotoxicity.

HIV-1 infected cells were labeled with a fluorescent reagent, Calcein-AM, and then incubated with noninfected MT-2 cells in 96-well plates in the presence or absence of the compounds being tested. After incubating for 2 h, the fused and unfused calcein-labeled HIV-1-infected cells were counted under an inverted fluorescence microscope, and the percent inhibition of cell–cell fusion and the IC₅₀ values were calculated. The inhibitory activity of compounds on infection by laboratory-adapted HIV-1 strains was determined by the p24 assay.³⁵ In brief, MT-2 cells were infected with HIV-1 in the presence or absence of compounds at graduated concentrations overnight. Culture supernatants were collected later from each well, mixed with equal volumes of 5% Triton X-100 and assayed for p24 antigen, which was quantitated by ELISA.³⁶

As shown in Table 1, all 10 compounds inhibited gp41 six-helix bundle formation in a dose-dependent manner, with IC₅₀ values ranging from 23 to 47 μM. Compounds **1004** and **2D6** inhibited HIV-1-mediated cell–cell fusion, and compounds **1032**, **2278**, **2249**, **2261**, and **1004** blocked HIV-1 replication at micromolar levels (Table 1).

Discussion

With the increasing rate of HIV infection worldwide, the development of effective anti-HIV-1 agents is of vital

importance. To date, 20 anti-HIV-1 drugs have been licensed by the U.S. Food and Drug Administration.³⁷ With the exception of Fuzeon, most anti-HIV drugs target HIV-1 protease and reverse transcriptase. The identification of molecules targeting viral entry has, therefore, opened a new avenue in the development of novel anti-HIV-1 therapeutics. Cell-permeable small molecules are of particular interest, since it is widely acknowledged that small molecules generally afford better oral availability, pharmacokinetics, and lower production cost than peptide-based drugs.

We have recently developed a strategy to disrupt protein–protein interactions using “credit card”-like compounds.²⁴ The structural stability of protein–protein interactions derives from large (typically 1000–3000 Å²), relatively shallow interfaces. The difficulty of disrupting such expansive interactions with small molecules may be due to (1) the extensively buried surface area on each side of the interface, as well as (2) the lack of deep small cavities that resemble small-molecule-binding sites, as seen from X-ray crystal structures.^{38,39} However, breakthroughs in breaching protein–protein interactions have occurred with the identification of “hot spots”. Hot spot domains have been characterized as shallow loci of ~600 Å² found at or near the geometric center of the protein–protein interface. These areas are generally characterized as being rich in aromatic residues, such as

tryptophan, tyrosine, and histidine. In addition, for many protein–protein interactions, the interface complementarity involves a significant level of protein flexibility and adaptivity.²⁶ There may be binding-site conformations that are well-suited to small molecule binding and that are not clearly visible in a single crystal structure. In total, it seems plausible that small, planar, aromatic scaffolds with appended diversity may be able to specifically access these hot spots and, thus, disrupt stabilizing interactions.

As the name implies, the credit card library members are simply planar, aromatic core structures adorned with chemical diversity. The compounds are intended to function as inhibitors of protein–protein interactions or otherwise alter the necessary interactions at the interface. From these libraries, compounds have been identified as inhibitors that disrupt Myc/Max oncoprotein dimerization, and with the aid of computational refinement, we have also identified compounds from the same libraries that inhibit the peripheral anionic binding site of acetylcholinesterase and reduce the ability of the β -amyloid peptide to aggregate and form fibrils.

The recent identification of a “hot spot” in the fusogenic form of gp41, namely, the deep hydrophobic pocket in the groove on the surface of the gp41 internal trimer formed by the NHR domains,^{1,40,41} inspired us to test our library against this target to identify molecules with a potential to disrupt this protein assembly. By employing a series of high-throughput screening (HTS) assays, Jiang and colleagues have identified a number of small-molecule HIV-1 fusion inhibitors that may dock in the gp41 hydrophobic pocket and block the gp41 six-helix bundle formation, for example, ADS-J1, NB-2, and NB-64.^{22,42} In the present study, we used this same series of high-throughput screening methods to select small molecule inhibitors from our credit card libraries. We first examined our two libraries with a sandwich ELISA using a unique mAb NC-1 which specifically recognizes the gp41 core formed by the NHR and CHR or the N- and C-peptides. This assay is optimized to be highly sensitive to allow the identification of compounds with minimal inhibitory activity. However, because of its extreme sensitivity, compounds with false-positive activity may also be selected, but these will eventually be excluded in a panel of secondary assays using ELISA, FN–PAGE, N–PAGE, etc.^{43,44} In the present study, we corroborated the sandwich ELISA results using a syncytium-formation assay to screen for compounds that inhibit HIV-1-induced membrane fusion.²² Though this assay is not quantitative, it is a sensitive cell-based screening method complementary to the cell-free sandwich ELISA assay. By utilizing these two HTS assays, we identified 10 compounds with inhibitory activity in one or both assays. These preselected compounds were further examined for their inhibitory activity on gp41 six-helix bundle formation, HIV-1-mediated cell fusion, and HIV-1 replication using quantitative assays under more stringent experimental conditions. Several of these preselected compounds exhibited inhibitory activity in a dose-dependent manner in all of these assays. Of these positive “hits”, five compounds, **1032**, **2278**, **2249**, **2261**, and **1004**, inhibited 6-helix bundle formation and viral antigen p24 production at low micromolar concentrations, and compound **1004** also inhibited cell–cell fusion at the

low micromolar level. To complete these studies, we also tested the in vitro cytotoxicity of these compounds to determine their selective index (SI) values; the results have been summarized in Table 1. The selective index value, defined as CC_{50}/IC_{50} , has previously been used as a general measurement of the anti-HIV-potency for peptide and small molecule inhibitors.¹⁰ Using similar HTS assay protocols, two compounds have been reported in the literature, namely, ADS-J1, with an SI value of 35.24, and ADS-J2, with an SI value of 9.43. In our study, compound **2261**, identified from credit-card library I, displayed an SI value of 4.2 and, thus, is our most promising compound for future sublibrary development for improvement of the SI value determined.

Conclusion

Protein–protein interactions are involved in most cellular processes and are of critical importance. On the basis of the nature of known protein–protein interactions and the recent identification of “hot spots” located at protein–protein interfaces, we hypothesized that small, planar, aromatic scaffolds with appended diversity may access specific areas at protein–protein interfaces and thus disrupt such interactions. To this end, we have prepared two small-molecule libraries, termed “credit card” libraries. From library I, multiple chemical entities were uncovered as Myc/Max dimerization inhibitors as well as compounds that inhibit the peripheral anionic binding site of acetylcholinesterase and reduce the ability of the β -amyloid peptide to aggregate and form fibrils. Inspired by the recently described “hot spot” located at the N-terminus of HIV-1 fusion protein gp41, we examined the same libraries in an effort to uncover molecules that inhibit the gp41 fusogenic transformation process.

Using several HTS assays, five compounds, **1032**, **2278**, **2249**, **2261**, and **1004**, were identified that inhibit six-helix bundle formation and viral antigen p24 production at low micromolar concentrations, and compound **1004** also inhibited cell–cell fusion at the low micromolar level. Although the anti-HIV-1 potencies (as evaluated by SI value) of the molecules identified from our studies are not therapeutically viable to be considered as drug candidates, these results provide a valuable class of new lead structures for designing more potent sublibraries that target the cell entry process.

Experimental Section

General Procedures. The ¹H NMR and ¹³C NMR spectra were recorded on either a Bruker AMX-400 or a Varian Inova-400 instrument. The following abbreviations were used to explain the multiplicities: s = singlet, d = doublet, t = triplet, q = quartet, m = multiplet, b = broad. High-resolution mass spectra (HRMS) were recorded at The Scripps Research Institute on a VG ZAB-ZSE mass spectrometer using MALDI. All reactions were monitored by thin-layer chromatography (TLC) carried out on 0.25-mm E. Merck silica gel plates (60F-254), with fractions being visualized by UV light. Column chromatography was carried out with Mallinckrodt SilicAR 60 silica gel (40–60 μ M). Reagent grade solvents for chromatography were obtained from Fisher Scientific. Reagents were purchased at the

highest commercial quality and used without further purification. All reactions were carried out under an argon atmosphere, unless otherwise noted. Reported yields were determined after purification for a homogeneous material.

6-(Benzyloxy)-2-naphthaldehyde and *tert*-Butyl 2-(6-formylnaphthalen-2-yloxy)acetate (2a and 2b). To a stirring solution of 6-hydroxy-2-naphthaldehyde (1.00 g, 5.8 mmol) and K_2CO_3 (4.0 g, 29 mmol) in DMF (30 mL), either benzyl chloride (6.4 mmol) or *tert*-butyl bromoacetate (0.87 mL, 6.4 mmol) was added, and the solution was stirred at 80 °C. After 2 h, the mixture was diluted with EtOAc (200 mL) and water (300 mL). The phases were separated, and the aqueous layer was washed with EtOAc (200 mL). The combined organics were washed with water, then brine, and dried over $MgSO_4$. Filtration, followed by concentration in vacuo, returned the product as a white solid, which was used without further purification:

6-(Benzyloxy)-2-naphthaldehyde (2a). 1H NMR (500 MHz, $CDCl_3$) δ 10.10 (s, 1H), 8.26 (s, 1H), 7.91 (m, 2H), 7.80 (d, $J = 8.5$ Hz, 1H), 7.38 (m, 7H), 5.15 (s, 2H). ^{13}C NMR (100 MHz, $CDCl_3$) δ 191.99, 167.63, 160.11, 159.87, 138.64, 134.65, 132.84, 131.58, 128.69, 128.22, 124.05, 120.74, 107.80, 70.46, 55.75. ESI-TOF calcd. $C_{18}H_{15}O_2$ [$M + H^+$], 263.1067; found, 263.1061.

***tert*-Butyl 2-(6-formylnaphthalen-2-yloxy)acetate (2b).** 1H NMR (500 MHz, $CDCl_3$) δ 8.33 (s, 1H), 7.99 (m, 2H), 7.84 (d, $J = 8.5$ Hz, 1H), 7.38 (dd, $J = 9.0, 2.5$ Hz, 1H), 7.18 (d, $J = 2.5$ Hz, 1H), 4.75 (s, 2H), 1.59 (s, 9H). ^{13}C NMR (125 MHz, $CDCl_3$) δ 192.3, 167.8, 158.6, 138.2, 134.5, 132.8, 131.6, 128.9, 128.5, 123.9, 120.0, 109.7, 107.5, 83.5, 65.9, 28.3. ESI-TOF calcd. $C_{17}H_{19}O_4$ [$M + H^+$], 287.1278; found, 287.1274.

7-Chloro-4-iodoquinoline (4). To a solution of 4,7-dichloroquinoline (12.0 g, 606 mmol) in propionitrile was added iodotrimethylsilane (25.0 g, 1.21 mmol) immediately out of its ampule, and a small amount of sodium iodide (0.5 g, 3.3 mmol). The resulting orange suspension was heated to reflux at 90° C. After 10 h, the reaction was transferred to a separatory funnel and quenched with water (400 mL) and 1 M sodium hydroxide (400 mL). After vigorous shaking to separate phases, the aqueous layer was washed with EtOAc (3 × 50 mL). The combined organic layers were then washed with water (1 × 100 mL) and brine (1 × 100 mL), then dried over $MgSO_4$. After filtration and concentration in vacuo, the yellow solid was crystallized in EtOAc/hexanes to give the product as white needles. Obtained = 14.9 g, 85% yield. 1H NMR (300 MHz, $CDCl_3$) δ 8.39 (d, $J = 4.5$ Hz, 1H), 8.00 (d, $J = 2.1$ Hz, 1H), 7.92 (d, $J = 4.5$ Hz, 1H), 7.88 (d, $J = 9.0$ Hz, 1H), 7.49 (dd, $J = 9.0, 2.1$ Hz, 1H). ^{13}C NMR (75 MHz, $CDCl_3$) δ 150.6, 148.0, 136.3, 133.0, 132.6, 129.0, 128.7, 111.4. ESI-TOF calcd. C_9H_6NClI [$M + H^+$], 289.9228; found, 289.9226.

7-Chloroquinoline-4-carbaldehyde (5). A 250-mL Schlenk flask charged with 7-chloro-4-iodoquinoline (5.18 g, 179 mmol) was vacuum-purged three times with argon, then dry THF (100 mL) was added via syringe. The solution was then cooled to -78° C with acetone/ CO_2 , and 1.6 M *n*-BuLi (16.8 mL, 268 mmol) was added all at once via syringe. The resulting black solution was stirred 4 min, then

anhydrous DMF (1.31 g, 179 mmol) was added all at once via syringe. The cooling bath was removed after 15 min and the reaction was allowed to warm to room temperature. After 2 h, the orange solution was quenched with water (50 mL). The reaction was transferred to a separatory funnel and washed with EtOAc (3 × 50 mL). The combined organic fractions were then washed with water (1 × 100 mL) and then brine (1 × 100 mL) then were dried over $MgSO_4$. After filtration, the solution was concentrated in vacuo, purified via flash chromatography (eluent 1:3 EtOAc/hexanes), and concentrated once more to a tan solid. Obtained = 2.45 g, 72% yield. 1H NMR (300 MHz, $CDCl_3$) δ 10.39 (s, 1H), 9.16 (d, $J = 4.2$ Hz, 1H), 8.92 (d, $J = 9.0$, 1H), 8.13 (d, $J = 2.1$, 1H), 7.73 (d, $J = 4.2$, 1H), 7.61 (dd, $J = 9.0$ Hz, $J = 2.1$ Hz, 1H). ^{13}C NMR (75 MHz, $CDCl_3$) δ 192.52, 151.5, 149.5, 136.6, 136.1, 130.1, 128.7, 126.1, 125.9, 121.9. ESI-TOF calcd. $C_{10}H_7ONCl$ [$M + H^+$], 192.0211; found, 192.0209.

General Procedure for Ugi Four-Component Condensations. To a solution of the naphthal derivative **2** (0.2 mmol, 1.0 equiv) in MeOH were added acid (0.4 mmol, 2.0 equiv), amine (0.4 mmol, 2.0 equiv), and isocyanide (0.4 mmol, 2.0 equiv). After stirring for 24 h at reflux, the mixture was cooled to room temperature and concentrated in vacuo. The residue was purified by a short silica gel column packed in a 5-mL Teflon syringe with 10–50% EtOAc/hexane gradient to afford the desired product. All products were analyzed by 1H NMR and HRMS. Compounds **1046**, **2293**, and **2300** are derived from corresponding *tert*-butyl esters of the Ugi products by TFA deprotection.

2-(6-(Benzyloxy)naphthalen-2-yl)-*N*-*tert*-butyl-2-(*N*-butyl-2-methoxyacetamido)acetamide (1004). 1H NMR (500 MHz, $CDCl_3$) δ 7.92 (s, 1H), 7.81(m, 2H), 7.57 (apparent d, $J = 7.0$ Hz, 2H), 7.48 (apparent td, $J = 7.5, 2.0$ Hz, 2H), 7.44 (m, 2H), 7.32 (m, 2H), 6.50 (s, 1H), 5.96 (s, 1H), 5.27 (s, 2H), 4.32 (d, $J = 14.0$ Hz, 1H), 4.23 (d, $J = 14$ Hz, 1H), 3.56 (s, 3H), 3.38 (m, 2H), 1.61 (m, 2H), 1.58 (m, 2H), 1.43 (s, 9H), 0.74 (t, $J = 7.3$ Hz, 3H). ^{13}C NMR (125 MHz, $CDCl_3$) δ 170.0, 169.9, 157.4, 136.7 (2 × ArC), 134.1, 130.4, 129.7, 128.7, 128.6 (3 × ArCH), 128.1, 127.5 (2 × ArCH), 127.3, 119.6, 106.9, 71.9, 70.0, 62.9, 59.1, 45.8, 38.5, 31.7, 28.6, 20.0, 13.6. ESI-TOF calcd. $C_{30}H_{39}N_2O_4$ [$M + H^+$], 491.2904; found, 491.2901.

***N*-(1-(6-(Benzyloxy)naphthalen-2-yl)-2-(*tert*-butylamino)-2-oxoethyl)-*N*-(2-methoxyethyl)butyramide (1032).** 1H NMR (600 MHz, $CDCl_3$) δ 7.51 (m, 11H), 6.01 (s, 1H), 5.17 (s, 2H), 3.44 (m, 3H), 3.10 (m, 4H), 2.48 (m, 2H), 1.69 (m, 2H), 1.34 (s, 9H), 0.95 (m, 3H). ^{13}C NMR (150 MHz, $CDCl_3$) δ 174.7, 169.3, 157.2, 136.6, 134.0, 130.8, 129.7, 128.7, 128.6 (2 × ArCH), 128.5, 128.0, 127.5 (2 × ArCH), 127.4, 127.3, 119.5, 106.8, 70.8, 69.9, 62.8, 58.5, 51.4, 45.7, 35.3, 28.6, 18.6, 13.8. ESI-TOF calcd. $C_{30}H_{39}N_2O_4$ [$M + H^+$], 491.2904; found, 491.2906.

***tert*-Butyl 2-(6-(1-(*N*-Butylpicolinamido)-2-(cyclohexylamino)-2-oxoethyl)naphthalen-2-yloxy)acetate.** 1H NMR (600 MHz, $CDCl_3$) δ 8.54 (s, 1H), 8.28 (s, 1H), 7.91 (s, 1H), 7.63 (m, 4H), 7.26 (m, 2H), 6.89 (m, 1H), 5.98 (s, 1H), 4.59 (s, 2H), 3.83 (m, 2H), 3.35 (m, 1H), 1.45 (m, 21 H), 0.80 (t, $J = 6.9$ Hz, 3H), 0.45 (m, 2H). ^{13}C NMR (150 MHz,

CDCl_3) δ 168.6, 167.7, 160.1, 156.1, 153.9, 148.2, 146.9, 137.8, 136.8, 133.8, 130.8, 129.7, 128.5, 127.2, 126.6, 124.9, 118.8, 106.6, 82.3, 65.6, 60.2, 47.9, 45.5, 32.8, 32.5, 31.4, 29.5, 28.0, 25.4, 24.4, 20.6, 14.0. ESI-TOF calcd. $\text{C}_{34}\text{H}_{44}\text{N}_3\text{O}_5$ [$\text{M} + \text{H}^+$], 574.3275; found, 574.3271.

2-(6-(1-(*N*-Butylpicolinamido)-2-(cyclohexylamino)-2-oxoethyl)naphthalen-2-yloxy)acetic Acid (1046). ^1H NMR (600 MHz, $\text{MeOD}-d_3$) δ 8.6 (s, 1H), 8.44 (d, $J = 4.8$ Hz, 1H), 8.21 (m, 1H), 7.44 (m, 7H), 5.98 (s, 1H), 5.84 (s, 1H), 4.60 (s, 2H), 3.52 (m, 1H), 3.14 (m, 1H), 2.82 (m, 1H), 0.97 (m, 17H). ^{13}C NMR (150 MHz, $\text{MeOD}-d_3$) δ 172.3, 160.3, 157.9, 154.7, 148.9, 139.9, 135.5, 130.8, 130.6, 128.4, 126.2, 120.2, 117.6, 115.7, 107.8, 65.6, 64.3, 48.3, 33.4 ($\times 2$), 31.7, 28.8, 25.7 ($\times 2$), 20.6, 13.3. ESI-TOF calcd. $\text{C}_{30}\text{H}_{36}\text{N}_3\text{O}_5$ [$\text{M} + \text{H}^+$], 518.2649; found, 518.2654.

***tert*-Butyl 2-(6-(2-(Cyclohexylamino)-1-(*N*-(4-methoxybenzyl)acetamido)-2-oxoethyl)naphthalen-2-yloxy)acetate (2249).** ^1H NMR (600 MHz, $\text{MeOD}-d_3$) δ 7.55 (m, 3H), 7.12 (m, 3H), 6.70 (apparent d, $J = 8.4$ Hz, 2H), 6.43 (apparent d, $J = 8.4$ Hz, 2H), 6.11 (s, 1H), 4.64 (d, $J = 16.8$ Hz, 1H), 4.61 (s, 2H), 4.43 (d, $J = 16.8$ Hz, 1H), 3.65 (s, 1H), 3.59 (s, 3H), 2.14 (s, 3H), 1.66 (m, 4H), 1.42 (s, 9H), 1.18 (m, 6H). ^{13}C NMR (150 MHz, $\text{MeOD}-d_3$) δ 174.7, 171.2, 169.5, 159.5, 157.5, 135.1, 131.3, 130.6, 130.3, 130.1, 129.8, 129.4, 128.5, 127.7 ($\times 2$), 119.6, 114.2, 113.7, 107.5, 80.1, 66.2, 63.5, 55.2, 49.7, 49.0, 33.1, 27.9, 26.2, 25.7. ESI-TOF calcd. $\text{C}_{34}\text{H}_{43}\text{N}_2\text{O}_6$ [$\text{M} + \text{H}^+$], 575.3115; found, 575.3110.

***tert*-Butyl 2-(6-(2-(Benzylamino)-1-(*N*-(4-methoxybenzyl)butyramido)-2-oxoethyl)naphthalen-2-yloxy)acetate (2261).** ^1H NMR (600 MHz, $\text{MeOD}-d_3$) δ 7.51 (m, 3H), 7.15 (m, 6H), 6.96 (m, 6H), 6.16 (s, 1H), 4.64 (d, $J = 17.4$ Hz, 1H), 4.56 (s, 2H), 4.31 (m, 3H), 3.55 (s, 3H), 2.36 (m, 1H), 2.21 (m, 1H), 1.57 (m, 2H), 1.41 (s, 9H), 0.82 (t, $J = 7.5$ Hz, 3H). ^{13}C NMR (150 MHz, $\text{MeOD}-d_3$) δ 177.4, 172.7, 170.0, 159.9, 157.8, 139.7, 135.5, 132.7, 131.4, 131.1, 130.8, 130.1, 129.9, 129.6, 129.5 ($\times 2$), 129.3, 128.5, 128.2 ($\times 2$), 128.1, 120.1, 114.9, 114.6, 107.9, 83.5, 66.6, 64.2, 55.6, 49.9, 44.1, 36.9, 28.3, 19.6, 14.3. ESI-TOF calcd. $\text{C}_{37}\text{H}_{43}\text{N}_2\text{O}_6$ [$\text{M} + \text{H}^+$], 611.3115; found, 611.3098.

***tert*-Butyl 2-(6-(2-(Cyclohexylamino)-1-(*N*-(2-methoxyethyl)-2-(4-methoxyphenyl)acetamido)-2-oxoethyl)naphthalen-2-yloxy)acetate (2278).** ^1H NMR (600 MHz, CDCl_3) δ 7.79 (m, 1H), 7.66 (m, 2H), 7.38 (m, 1H), 7.21 (m, 3H), 7.03 (m, 1H), 6.87 (m, 2H), 5.96 (s, 1H), 4.62 (s, 2H), 3.81 (m, 5H), 3.60 (m, 1H), 3.43 (m, 1H), 3.32 (s, 2H), 3.16 (s, 3H), 3.09 (m, 1H), 1.42 (m, 19H). ^{13}C NMR (150 MHz, $\text{MeOD}-d_3$) δ 168.7, 167.8, 160.2, 158.4, 156.4, 133.8, 130.8, 130.0 ($2 \times \text{ArCH}$), 129.9, 129.0, 128.4, 127.5, 127.3, 127.1, 119.1, 114.2, 114.0, 106.7, 82.5, 70.9, 65.7, 62.9, 58.8, 55.2, 48.5, 46.2, 39.9, 33.2, 32.9, 28.0, 25.4, 25.1, 24.7. ESI-TOF calcd. $\text{C}_{36}\text{H}_{47}\text{N}_2\text{O}_7$ [$\text{M} + \text{H}^+$], 619.3378; found, 619.3393.

***tert*-Butyl 2-(6-(1-(*N*-Butyl-2-methoxyacetamido)-2-(*tert*-butylamino)-2-oxoethyl)naphthalen-2-yloxy)acetate.** ^1H NMR (600 MHz, CDCl_3) δ 7.81 (s, 1H), 7.71 (d, $J = 9.0$ Hz, 1H), 7.65 (d, $J = 8.4$ Hz, 1H), 7.39 (d, $J = 7.8$ Hz, 1H), 7.21 (dd, $J = 9.0, 2.4$ Hz, 1H), 7.01 (d, $J = 1.8$ Hz, 1H), 5.83 (s, 1H), 4.60 (s, 2H), 4.20 (d, $J = 14.4$ Hz, 1H), 4.12 (d, $J = 14.4$ Hz, 1H), 3.44 (s, 3H), 3.23 (m, 2H), 1.46

(s, 9H), 1.32 (overlapping s and m, 11H), 0.96 (m, 2H), 0.61 (t, $J = 7.2$ Hz, 3H). ^{13}C NMR (150 MHz, CDCl_3) δ 171.0, 169.2, 167.7, 156.3, 133.8, 130.7, 129.8, 128.9, 128.6, 127.5, 127.3, 119.1, 106.7, 82.4, 71.0, 65.6, 62.7, 60.3, 59.0, 51.3, 45.6, 28.8, 28.5, 27.9, 19.9, 13.2. ESI-TOF calcd. $\text{C}_{29}\text{H}_{43}\text{N}_2\text{O}_6$ [$\text{M} + \text{H}^+$], 515.3115; found, 515.3112.

2-(6-(1-(*N*-Butyl-2-methoxyacetamido)-2-(*tert*-butylamino)-2-oxoethyl)naphthalen-2-yloxy)acetic Acid (2293). ^1H NMR (500 MHz, $\text{MeOD}-d_3$) δ 7.70 (m, 3H), 7.33 (dd, $J = 8.5, 1.5$ Hz, 1H), 7.16 (m, 2H), 5.94 (s, 1H), 5.70 (s, 1H), 4.71 (s, 2H), 4.15 (m, 2H), 3.32 (s, 3H), 3.15 (t, $J = 7.4$ Hz, 2H), 1.25 (s, 9H), 0.82 (m, 4H), 0.44 (t, $J = 7.0$ Hz, 3H). ^{13}C NMR (125 MHz, $\text{MeOD}-d_3$) δ 172.6, 171.0, 164.1, 158.3, 135.8, 132.2, 130.9, 130.5, 130.4, 129.3, 128.7, 120.6, 108.2, 72.8, 66.1, 64.2, 59.7, 52.5, 46.4, 29.1, 27.8, 21.0, 13.9. ESI-TOF calcd. $\text{C}_{25}\text{H}_{35}\text{N}_2\text{O}_6$ [$\text{M} + \text{H}^+$], 459.2490; found, 459.2485.

***tert*-Butyl 2-(6-(2-(Benzylamino)-1-(*N*-butyl-2-methoxyacetamido)-2-oxoethyl)naphthalen-2-yloxy)acetate.** ^1H NMR (600 MHz, CDCl_3) δ 7.80 (s, 1H), 7.68 (d, $J = 9.0$ Hz, 1H), 7.65 (d, $J = 8.4$ Hz, 1H), 7.40 (d, $J = 7.8$ Hz, 1H), 7.26 (m, 5H), 7.02 (s, 1H), 6.63 (s, 1H), 5.96 (s, 1H), 4.61 (s, 2H), 4.21 (d, $J = 13.8$ Hz, 1H), 4.15 (d, $J = 14.4$ Hz, 1H), 4.00 (s, 3H), 3.41 (s, 3H), 3.29 (m, 2H), 1.47 (s, 9H), 1.38 (m, 1H), 0.99 (m, 3H), 0.63 (t, $J = 6.9$ Hz, 3H). ^{13}C NMR (150 MHz, CDCl_3) δ 170.7, 168.1, 162.1, 156.7, 138.1, 134.2, 130.3, 130.1, 129.2, 129.0, 128.8, 127.9, 127.8, 127.7, 127.6, 119.5, 107.0, 82.8, 71.1, 69.5, 63.4, 59.5, 46.5, 43.9, 31.8, 28.3, 20.1, 13.6. ESI-TOF calcd. $\text{C}_{32}\text{H}_{41}\text{N}_2\text{O}_6$ [$\text{M} + \text{H}^+$], 549.2959; found, 549.2954.

2-(6-(2-(Benzylamino)-1-(*N*-butyl-2-methoxyacetamido)-2-oxoethyl)naphthalen-2-yloxy)acetic Acid (2300). ^1H NMR (600 MHz, $\text{MeOD}-d_3$) δ 7.70 (d, $J = 8.4$ Hz, 1H), 7.64 (m, 1H), 7.33 (m, 2H), 7.16 (m, 7H), 6.04 (s, 1H), 4.70 (s, 2H), 4.23 (m, 2H), 3.92 (s, 2H), 3.32 (s, 3H), 3.14 (m, 2H), 1.22 (m, 1H), 0.76 (m, 3H), 0.42 (t, $J = 7.2$ Hz, 3H). ^{13}C NMR (150 MHz, $\text{MeOD}-d_3$) δ 174.0, 172.6, 172.5, 158.1, 139.9, 135.6, 131.4, 130.8, 130.5, 130.3, 129.9, 129.6, 129.5, 128.7, 120.4, 107.9, 70.1, 65.8, 64.0, 59.5, 46.1, 44.3, 31.1, 20.8, 13.6. ESI-TOF calcd. $\text{C}_{28}\text{H}_{33}\text{N}_2\text{O}_6$ [$\text{M} + \text{H}^+$], 493.2333; found, 493.2334.

2-(6-(Benzoyloxy)naphthalen-2-yl)-*N*-cyclohexyl-2-(*N*-(2-methoxyethyl)-2-(4-methoxyphenyl)acetamido)acetamide (299). ^1H NMR (600 MHz, CDCl_3) δ 7.39 (m, 15H), 5.94 (s, 1H), 5.14 (s, 2H), 3.79 (overlapping s and m, 5H), 3.58 (m, 1H), 3.42 (m, 1H), 3.30 (s, 2H), 3.13 (s, 3H), 3.06 (m, 1H), 1.46 (m, 10H). ^{13}C NMR (150 MHz, CDCl_3) δ 173.2, 168.9, 158.4, 157.3, 136.6, 134.1, 130.5, 129.9 ($2 \times \text{ArCH}$), 129.7, 128.7, 128.6 ($2 \times \text{ArCH}$), 128.4, 128.0, 127.5 ($2 \times \text{ArCH}$), 127.4, 127.3, 127.0, 119.6, 114.2, 114.0, 106.9, 70.9, 70.0, 66.4, 58.2, 55.2, 48.5, 46.2, 41.0, 33.1, 33.0, 30.9, 25.3, 24.7. ESI-TOF calcd. $\text{C}_{37}\text{H}_{43}\text{N}_2\text{O}_5$ [$\text{M} + \text{H}^+$], 595.3166; found, 595.3161.

2-(7-Chloroquinolin-4-yl)-*N*-cyclohexyl-2-hydroxyacetamide (2D6). ^1H NMR (300 MHz, CDCl_3) δ 8.91 (d, $J = 2.2$ Hz, 1H), 8.84 (d, $J = 4.6$ Hz, 1H), 8.27 (d, $J = 4.6$ Hz, 1H), 7.93 (d, $J = 4.6$ Hz, 1H), 7.76 (d, $J = 2.2$ Hz, 1H), 5.92 (s, 1H), 3.40 (m, 1H), 1.90–1.10 (m, 10H). ^{13}C NMR (300 MHz, CDCl_3) δ 170.2, 158.4, 152.5, 141.8, 136.9,

132.8, 129.5, 128.4, 128.1, 122.6, 72.0, 55.9, 35.4, 26.7, 25.6. ESI-TOF calcd. $C_{17}H_{19}ClN_2O_2$ [$M + H^+$], 319.1135; found, 319.1130.

Sandwich ELISA for Screening for Inhibitors of the gp41 Core Formation. A sandwich ELISA as previously described³⁰ was used to screen for compounds that inhibit the gp41 six-helix bundle formation. Briefly, peptide N36 (2 μ M) was preincubated with a test compound at the indicated concentrations at 37 °C for 30 min, followed by addition of C34 (2 μ M). After incubation at 37 °C for 30 min, the mixture was added to wells of a 96-well polystyrene plate (Costar, Corning Inc., Corning, NY), which were precoated with IgG (2 μ g/mL) purified from rabbit antisera directed against the N36/C34 mixture. Then, the mAb NC-1, biotin-labeled goat anti-mouse IgG (Sigma Chemical Co., St. Louis, MO), streptavidin-labeled horseradish peroxidase (SA-HRP) (Zymed, S. San Francisco, CA), and the substrate 3,3',5,5'-tetramethylbenzidine (TMB) (Sigma) were added sequentially. Absorbance at 450 nm was measured using an ELISA reader (Ultra 384, Tecan, Research Triangle Park, NC). The percent inhibition by the compounds was calculated as previously described.³⁵

Screening for HIV-1 Fusion Inhibitors by Syncytium-Formation Assay. HIV-1_{IIIIB}-infected H9 cells (H9/HIV-1_{IIIIB}) at 2×10^5 /mL were cocultured with MT-2 cells (2×10^6 /mL) in the presence of compounds to be screened (final concentration of compound: 25 μ g/mL) in a 96-well plate at 37 °C for 2 days. HIV-1-induced syncytium formation was observed under an inverted microscope and scored as “+” (no syncytium was observed), “±” (syncytium formation was partially inhibited), and “-” (syncytium formation was not inhibited). The compounds scored with “+” and “±” were selected for further study.

Measurement of the Inhibitory Activity of Compounds on the gp41 Six-Helix Bundle Formation. An enzyme immunoassay (EIA) was used for measuring the inhibitory activity of compounds on the gp41 six-helix bundle formation. Briefly, peptide N36 (2 μ M) was preincubated with a selected compound at graded concentrations at 37 °C for 30 min, followed by addition of biotinylated C34 (2 μ M) and incubation at 37 °C for 30 min. The mixture was added to wells of a 96-well polystyrene plate (Costar, Corning Inc., Corning, NY) which were precoated with the mAb NC-1. After incubation at 37 °C for 1 h, SA-HRP and TMB were added sequentially. Absorbance at 450 nm was measured as described above. The percent inhibition and the concentration for 50% inhibition (IC_{50}) was calculated using the software designated Calcsyn,⁴⁵ kindly provided by Dr. T. C. Chou (Sloan-Kettering Cancer Center, New York, NY).

Assessment of Inhibitory Activity of Compounds on HIV-1 Replication. The inhibitory activity of compounds on infection by laboratory-adapted HIV-1 strains was determined as previously described^{33,8}. In brief, 1×10^4 MT-2 cells were infected with HIV-1 at 100 TCID₅₀ (50% tissue culture infective dose) in 200 μ L of RPMI 1640 medium containing 10% FBS in the presence or absence of compounds at graded concentrations overnight. For the time-of-addition assay, compounds were added at various times postinfection. Then the culture supernatants were removed,

and fresh culture media were added. On the fourth day postinfection, 100 μ L of culture supernatants was collected from each well, mixed with equal volumes of 5% Triton X-100, and assayed for p24 antigen, which was quantitated by ELISA.³⁴ Briefly, the wells of polystyrene plates (Immulon 1B, Dynex Technology, Chantilly, VA) were coated with HIVIG in 0.085 M carbonate–bicarbonate buffer (pH 9.6) at 4 °C overnight, followed by washes with PBS-T buffer (0.01M PBS containing 0.05% Tween-20) and blocking with PBS containing 1% dry fatfree milk (Bio-Rad Inc., Hercules, CA). Virus lysates were added to the wells and incubated at 37 °C for 1 h. After extensive washes, anti-p24 mAb (183–12H-5C), biotin-labeled anti-mouse IgG1 (Santa Cruz Biotech., Santa Cruz, CA), SA-HRP, and TMB were added sequentially. Reactions were terminated by addition of 1 N H₂SO₄. Absorbance at 450 nm was recorded in an ELISA reader (Ultra 384, Tecan). Recombinant protein p24 (US Biological, Swampscott, MA) was included for establishing standard dose–response curves.

HIV-1-Mediated Cell–Cell Fusion. A dye transfer assay was used for detection of HIV-1 mediated cell–cell fusion as previously described.^{16,40} H9/HIV-1_{IIIIB} cells were labeled with a fluorescent reagent, Calcein-AM (Molecular Probes, Inc., Eugene, OR) and then incubated with MT-2 cells (ratio = 1:5) in 96-well plates at 37 °C for 2 h in the presence or absence of compounds tested. The fused and unfused calcein-labeled HIV-1-infected cells were counted under an inverted fluorescence microscope (Zeiss, Germany) with an eyepiece micrometer disk. The percent inhibition of cell–cell fusion and the IC_{50} values were calculated as previously described.¹⁶

Acknowledgment. We thank Drs. James Farmer and Jinkui Niu at the MicroChemistry Laboratory of the New York Blood Center for peptide synthesis. This work was supported by Skaggs Institute for Chemical Biology and NIH Grant RO1 AI46221 to S.J. We also thank the NIH AIDS Reagent Repository for providing HIV-1_{IIIIB}, MT-2 cells, HIV-1_{IIIIB} chronically infected H9 cells (H9/HIV-1_{IIIIB}), anti-p24 mAb (183-12H-5C), and HIV immunoglobulin (HIVIG).

References and Notes

- Chan, D. C.; Chutkowski, C. T.; Kim, P. S. *Proc. Natl. Acad. Sci. U.S.A.* **1998**, *95*, 15613–15617.
- Chan, D. C.; Fass, D.; Berger, J. M.; Kim, P. S. *Cell* **1997**, *89*, 263–273.
- Ketas, T. J.; Klasse, P. J.; Spennleauer, C.; Nesen, M.; Frank, I.; Pope, M.; Strizki, J. M.; Reyes, G. R.; Baroudy, B. M.; Moore, J. P. *AIDS Res. Hum. Retroviruses* **2003**, *19*, 177–186.
- Liu, S. W.; Jiang, S. B. *Curr. Pharm. Des.* **2004**, *10*, 1827–1843.
- Moore, J. P.; Doms, R. W. *Proc. Natl. Acad. Sci. U.S.A.* **2003**, *100*, 10598–10602.
- Fauci, A. S. *Nat. Med.* **2003**, *9*, 839–843.
- Pomerantz, R. J.; Horn, D. L. *Nat. Med.* **2003**, *9*, 867–873.
- Chan, D. C.; Kim, P. S. *Cell* **1998**, *93*, 681–684.
- Jiang, S.; Siddiqui, P.; Liu, S. *Drug Discovery Today: Therapeutic Strategies* **2004**, *1*, 497–503.
- Jiang, S. B.; Zhao, Q.; Debnath, A. K. *Curr. Pharm. Des.* **2002**, *8*, 563–580.
- Chen, S. S. L. *Intervirology* **1996**, *39*, 242–248.
- Sattentau, Q. J.; Moore, J. P.; Vignaux, F.; Traincard, F.; Poignard, P. *J. Virol.* **1993**, *67*, 7383–7393.

- (13) Berger, E. A.; Murphy, P. M.; Farber, J. M. *Annu. Rev. Immunol.* **1999**, *17*, 657–700.
- (14) Lu, M.; Kim, P. S. *J. Biomol. Struct. Dyn.* **1997**, *15*, 465–471.
- (15) Weissenhorn, W.; Dessen, A.; Harrison, S. C.; Skehel, J. J.; Wiley, D. C. *Nature* **1997**, *387*, 426–430.
- (16) Jiang, S. B.; Lin, K.; Strick, N.; Neurath, A. R. *Nature* **1993**, *365*, 113–113.
- (17) Wild, C.; Oas, T.; McDanal, C.; Bolognesi, D.; Matthews, T. J. *Cell. Biol.* **1993**, *222*–222.
- (18) Wild, C. T.; Shugars, D. C.; Greenwell, T. K.; McDanal, C. B.; Matthews, T. J. *Proc. Natl. Acad. Sci. U.S.A.* **1994**, *91*, 9770–9774.
- (19) Chen, R. Y.; Kilby, J. M.; Saag, M. S. *Expert Opin. Invest. Drugs* **2002**, *11*, 1837–1843.
- (20) Bianchi, E.; Finotto, M.; Ingallinella, P.; Hrin, R.; Carella, A. V.; Hou, X. S.; Schleif, W. A.; Miller, M. D.; Geleziunas, R.; Pessi, A. *Proc. Natl. Acad. Sci. U.S.A.* **2005**, *102*, 12903–12908.
- (21) Ferrer, M.; Kapoor, T. M.; Strassmaier, T.; Weissenhorn, W.; Skehel, J. J.; Oprian, D.; Schreiber, S. L.; Wiley, D. C.; Harrison, S. C. *Nat. Struct. Biol.* **1999**, *6*, 953–960.
- (22) Jiang, S. B.; Lu, H.; Liu, S. W.; Zhao, Q.; He, Y. X.; Debnath, A. K. *Antimicrob. Agents Chemother.* **2004**, *48*, 4349–4359.
- (23) Liu, S. W.; Lu, H.; Zhao, Q.; He, Y. X.; Niu, J. K.; Debnath, A. K.; Wu, S. G.; Jiang, S. B. *Biochim. Biophys. Acta* **2005**, *1723*, 270–281.
- (24) Xu, Y.; Shi, J.; Yamamoto, N.; Moss, J. A.; Vogt, P. K.; Janda, K. D. *Bioorg. Med. Chem.* **2005**, *14*, 2660–2673.
- (25) Dickerson, T. J.; Beuscher, A. E.; Hixon, M. S.; Yamamoto, N.; Xu, Y.; Olson, A. J.; Janda, K. D. *Biochemistry* **2005**, *44*, 14845–14853.
- (26) Bogan, A. A.; Thorn, K. S. *J. Mol. Biol.* **1998**, *280*, 1–9.
- (27) Berg, T. *ChemBioChem* **2004**, *5*, 1051–1053.
- (28) Ugi, I.; Meyr, R. *Angew. Chem.-Int. Ed.* **1958**, *70*, 702–703.
- (29) Domling, A.; Ugi, I. *Angew. Chem., Int. Ed.* **2000**, *39*, 3169–3210.
- (30) Jiang, S. B.; Lin, K.; Zhang, L.; Debnath, A. K. *J. Virol. Methods* **1999**, *80*, 85–96.
- (31) Passerini, M. *Gazz. Chim. Ital.* **1921**, *51*, 126.
- (32) Passerini, M. *Gazz. Chim. Ital.* **1921**, *51*, 181.
- (33) Jiang, S.; Boyer-Chatenet, L. *Antiviral Res.* **2002**, *53*, A69–A69.
- (34) Raviv, Y.; Viard, M.; Bess, J.; Blumenthal, R. *Virology* **2002**, *293*, 243–251.
- (35) Jiang, S.; Lin, K.; Neurath, A. R. *J. Exp. Med.* **1991**, *174*, 1557–1563.
- (36) Zhao, Q.; Ernst, J. T.; Hamilton, A. D.; Debnath, A. K.; Jiang, S. B. *AIDS Res. Hum. Retroviruses* **2002**, *18*, 989–997.
- (37) De Clercq, E. *Med. Chem. Res.* **2004**, *13*, 439–478.
- (38) Arkin, M. R.; Wells, J. A. *Nat. Rev. Drug Discovery* **2004**, *3*, 301–317.
- (39) Gadek, T. R.; Nicholas, J. B. *Biochem. Pharmacol.* **2003**, *65*, 1–8.
- (40) Ji, H.; Shu, W.; Burling, F. T.; Jiang, S. B.; Lu, M. *J. Virol.* **1999**, *73*, 8578–8586.
- (41) Zhou, G. F.; Ferrer, M.; Chopra, R.; Kapoor, T. M.; Strassmaier, T.; Weissenhorn, W.; Skehel, J. J.; Oprian, D.; Schreiber, S. L.; Harrison, S. C.; Wiley, D. C. *Bioorg. Med. Chem.* **2000**, *8*, 2219–2227.
- (42) Debnath, A. K.; Radigan, L.; Jiang, S. B. *J. Med. Chem.* **1999**, *42*, 3203–3209.
- (43) Liu, S. W.; Boyer-Chatenet, L.; Lu, H.; Jiang, S. B. *J. Biomol. Screening* **2003**, *8*, 685–693.
- (44) Liu, S. W.; Zhao, Q.; Jiang, S. B. *Peptides* **2003**, *24*, 1303–1313.
- (45) Chou, T. C.; Hayball, M. P. *CalcuSyn: Windows software for dose effect analysis*; BIOSOFT: Ferguson, MO 63135, 1991.